Geomechanics and Engineering, *Vol. 35, No. 4 (2023) 385-393*
https://doi.org/10.12989/gae.2023.35.4.385

Free-strain solutions for two-dimensional consolidation with sand blankets under multi-ramp loading

Zan Li*[1,2], Songyu Liu[1,2a] and Cuiwei Fu[3b]

[1]*Institute of Geotechnical Engineering, Southeast University, Nanjing 210096, China*
[2]*Jiangsu Key Laboratory of Urban Underground Engineering and Environmental Safety, Southeast University, Nanjing 210096, China*
[3]*China Railway First Survey and Design Institute Group Co., Ltd., Xi'an 710043, China*

(*Received July 29, 2022, Revised September 19, 2023, Accepted November 1, 2023*)

Abstract. To analyze the consolidation with horizontal sand drains, the plane strain consolidation model under multi-ramp loading is established, and its corresponding analytical solution is derived by using the separation of variables method. The proposed solution is verified by the field measurement data and finite element results. Then, the effects of the loading mode and stress distribution on consolidation and dissipation of pore pressure are investigated. At the same time, the influence of hydraulic conductivity and thickness of sand blankets on soil consolidation are also analyzed. The results show that the loading mode has a significant effect on both the soil consolidation rate and generation-dissipation process of pore water pressure. In contrast, the influence of stress distribution on pore pressure dissipation is obvious, while its influence on soil consolidation rate is negligible. To guarantee the fully drained condition of the sand blanket, the ratio of hydraulic conductivity of the sand blanket to that of clay layer k_d/k_v should range from 1.0×10^4 to 1.0×10^6 with soil width varying from 100 m to 1000 m. A larger soil width correspondingly needs a greater value of kd/kv to make sure that the pore water can flow through the sand blanket smoothly with little resistance. When the soil width is relatively small (e.g., less than 100 m), the effect of thickness of the sand blanket on soil consolidation is insignificant. And its influence appears obvious gradually with the increase of the soil width.

Keywords: consolidation; horizontal drainage; multi-ramp loading; sand blanket; plane strain

1. Introduction

In recent years, horizontal sand blankets have been widely used to accelerate the consolidation process, especially in the project of clay fill embankment (Gibson and Shefford 1968) and reclaimed land (Lee *et al*. 1987, Tan *et al*. 1992, Nogami and Li 2002, 2003, Jang and Mimura 2005, Mesri and Funk 2015, Feng *et al*. 2019). Therefore, it is particularly important to study the drainage efficiency of horizontal drains (Mesri 1973, Nogami and Li 2002, Lei *et al*. 2016, Ni *et al*. 2019, Yao *et al*. 2019, Tian *et al*. 2020).

As a conventional and crucial topic in geotechnical engineering, soil consolidation has always obtained the interest of many researchers. As a result, various analytical methods and numerical models have been developed to analyze the consolidation of ground with horizontal drainage. As the pioneering work, Gray (1945) first studied the soil consolidation problem of laying horizontal sand blanket on the foundation surface, considering the vertical seepage of sand blankets. However, the horizontal seepage of sand blanket was ignored. Then, Gibson and Shefford (1968) used the analytical method to analyze the efficiency of drainage layers to accelerate consolidation of clay fill embankments. The drainage efficiency was evaluated under three types of loading methods (i.e., constant loading, constant rate of loading and triangular loading). However, the horizontal flow in the clay and the effect of the thickness and length of the sand blanket on soil consolidation were neglected. Based on the Gibson and Shefford's solution, Tan *et al*. (1992) investigated the consolidation problem of a layered clay-sand scheme of land reclamation in which an intermediate sand layer is sandwiched by two layers of clay. It was found that the drainage efficiency of the system was controlled by a characteristic factor $\lambda = (k_s/k_c)\cdot(H/L)\cdot(H_s/L)$, which is composed of the permeability ratios of the sand to clay k_s/k_c, the flow-length ratio of the sand to clay H/L, and the ratio of the sand thickness to its horizontal length H_s/L. However, the results were only applicable to the equal thickness of clay between adjacent sand blankets. Subsequently, taking into account the unequal thickness of sand blankets and clay layers, Nogami and Li (2002) developed formulations to compute the consolidation behavior of a clay soil containing multiple thin sand layers. Similar results to that of Tan *et al*. (1992) were obtained, and a design criterion was proposed for designing multiple thin sand layers to accelerate the consolidation of a constructed clay ground.

Based on the plane strain unit cell theory, Chai *et al*. (2014) developed a method for the consolidation analysis of dredged mud or clayey soil deposits with horizontal drains. In addition, the material selection and thickness

*Corresponding author, Ph.D. Student
E-mail: lizan@seu.edu.cn
[a]Professor
[b]Ph.D.

ISSN: 2005-307X (Print), 2092-6219 (Online)

optimization of horizontal drains were also investigated in the literature (Chai and Miura 1999, Lee and Oda 2015). Recently, the contribution of soil's self-weight was taken into account when dealing with the consolidation problem in land reclamation with sand blankets for accelerating the consolidation process (Feng *et al*. 2019, 2020, 2021). However, only one-dimensional consolidation was considered in these literature, and the excess pore water pressure in horizontal sand layers was assumed to be zero. On the other hand, according to the in-situ monitoring data of Maishima, Yumeshima and Sakishima Reclaimed Islands in Osaka Port, the elasto-viscoplastic finite element method was carried out to evaluate the long-term settlement of the reclaimed islands (Mimura *et al*. 2003, Mimura and Jang 2004, 2005, Jang and Mimura 2005).

Actually, although the vertical flow in the clay dominates the consolidation process, horizontal and vertical seepages occur synchronously during the consolidation process, and it should be regarded as a two-dimensional consolidation problem. In addition, evidently, the hydraulic conductivity of sand blankets has an important influence on the consolidation efficiency. Therefore, a due attention should also be paid to the thickness and length of sand blankets which also controls the process of generation and dissipation of excess pore water pressure. However, there is no existing analytical solution to solve such a problem. In addition, the construction of clay fill embankment and reclaimed land is a long-term process and may continue to several months, even several years (Tan *et al*. 1992, Mimura *et al*. 2003, Mimura and Jang 2004, 2005, Jang and Mimura 2005). Therefore, the loading mode can be reasonably approximated as multi-ramp loading (Zhu and Yin 2004, Conte and Troncone 2006, Lu *et al*. 2011, Lei *et al*. 2015, 2016). Instantaneous or linear loading may lead to considerable differences in analyzing the process of excess pore water pressure and degree of consolidation. Therefore, it is an extremely challenging work to formulate a generalized solution to consider all these aspects of consolidation (i.e., multi-ramp loading, both horizontal and vertical seepage, length and width of the sand blanket) simultaneously using the analytical method.

To address this challenge, in this paper, an analytical solution for two-dimensional consolidation with sand blankets under multi-ramp loading is developed. Subsequently, the solution is verified using field measured data. Then, the effects of the loading mode and stress distribution on consolidation and dissipation of pore pressure are investigated using the proposed solution. Meanwhile, the influence of hydraulic conductivity and thickness of sand blankets on soil consolidation are also analyzed.

2. Problem description

Fig. 1 shows a plane strain consolidation model with horizontal sand drainage blankets on the bottom and top surfaces. As mentioned before, the soil is subjected to a depth-varying and time-dependent increase in total stress under multi-ramp loading. The governing equation of free-strain consolidation is given as follows

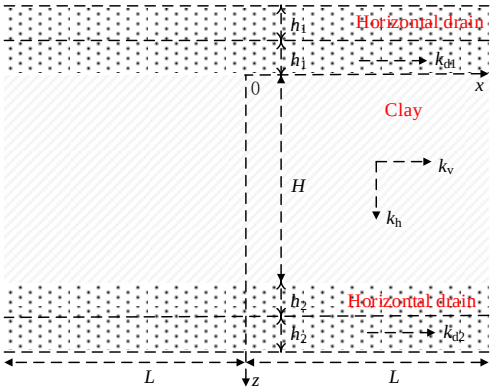

Fig. 1 Schematic diagram of ground consolidation problem with horizontal sand drainage blankets

$$\frac{k_h}{\gamma_w}\frac{\partial^2 u}{\partial x^2}+\frac{k_v}{\gamma_w}\frac{\partial^2 u}{\partial z^2}=-m_v\left(\frac{\partial \sigma}{\partial t}-\frac{\partial u}{\partial t}\right),\ 0\le x\le L \tag{1}$$

where x and z are the horizontal and vertical coordinates, respectively; t is time; u is the excess pore-water pressure of soil; L is the width of soil; σ is the increase in total stress in soil due to surcharge loading; k_h, k_v and m_v are the horizontal and vertical hydraulic conductivity and volume compressibility of the soil, respectively; and γ_w is the unit weight of water.

Considering the symmetry of the model, the drainage conditions on the midline and right sides of the soil can be described as

$$\frac{\partial u}{\partial x}=0,\ x=0 \tag{2}$$

$$u=0,\ x=L \tag{3}$$

Since the sand blanket is mainly drained horizontally, the vertical seepage can be neglected (Tan *et al*. 1992). In addition, the permeability coefficient of sand blanket is much larger than that of the soil to be consolidated. Therefore, it is reasonably assumed that pore water pressure in sand blanket is evenly distributed along the thickness (Gibson and Shefford 1968). Note that the compressibility of sand blanket is negligible compared with the soil layer to be consolidated. Similar to the establishment method of well resistance equation in the consolidation problem with vertical drains (Barron 1948, Indraratna *et al*. 2012, Liu *et al*. 2014, Lei *et al*. 2015, 2016, Li *et al*. 2016), the boundary conditions on the top and bottom of the soil layer to be consolidated can be obtained according to the seepage continuity conditions

$$\frac{k_v}{\gamma_w}\frac{\partial u}{\partial z}+\frac{k_{d1}h_1}{\gamma_w}\frac{\partial^2 u}{\partial x^2}=0,\ z=0 \tag{4}$$

$$\frac{k_v}{\gamma_w}\frac{\partial u}{\partial z}-\frac{k_{d2}h_2}{\gamma_w}\frac{\partial^2 u}{\partial x^2}=0,\ z=h \tag{5}$$

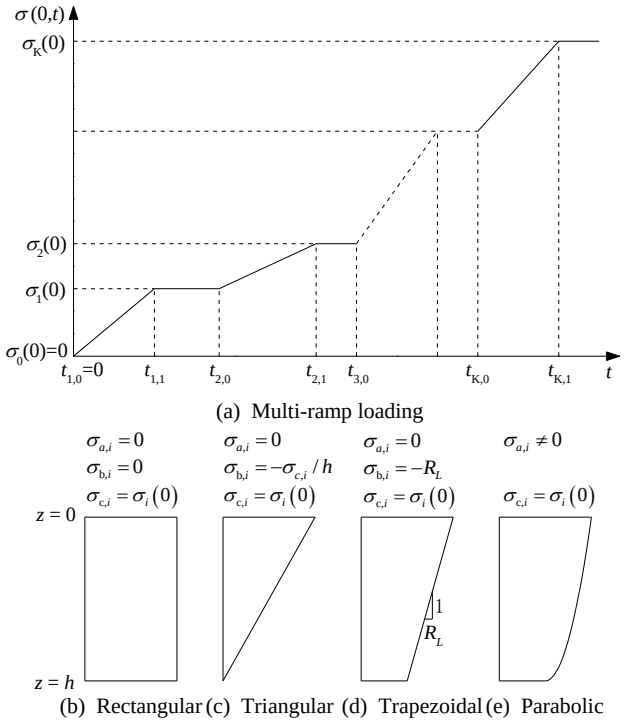

Fig. 2 Depth-varying and time-dependent increase in total stress in soil under multi-ramp loading

where k_{d1} and k_{d2} are the horizontal hydraulic conductivity of the horizontal sand blankets on the top and bottom of soil, respectively; h_1 and h_2 are the thicknesses of sand blankets on the top and bottom of soil, respectively; h is the thickness of consolidation soil.

Fig. 2 schematically shows the depth-varying increase in total stress in soil due to multi-ramp surcharge loading. To facilitate the derivation of the analytical solution, a new single equation is constructed to accurately describe the increase in total stress

$$\sigma(x,z,t)=\sum_{i=1}^{K}F_i(t)\left[\sigma_i(x,z)-\sigma_{i-1}(x,z)\right] \tag{6}$$

where

$$F_i(t)=\frac{t-t_{i,0}}{t_{i,1}-t_{i,0}}H\left\langle t-t_{i,0}\right\rangle\left[1-H\left\langle t-t_{i,1}\right\rangle\right]+H\left\langle t-t_{i,1}\right\rangle \tag{7}$$

$$\sigma_i(x,z)=\sigma_{a,i}z^2+\sigma_{b,i}z+\sigma_{c,i} \tag{8}$$

$$H\left\langle t-t_{i,j}\right\rangle=\begin{cases}0, & \left(t-t_{i,j}\right)<0\\ 1, & \left(t-t_{i,j}\right)\geq 0\end{cases}\quad(j=0,1) \tag{9}$$

The initial condition is given by

$$u=0,\ t=0 \tag{10}$$

where K is the total number of loading ramps; $t_{i,0}$ and $t_{i,1}$ are the start time and end time of the i-th ramp, respectively, as shown in Fig. 2(a); σ_i is the increase in total stress in soil at the end time of the i-th ramp, and $\sigma_0 = 0$; and $\sigma_{a,i}$, $\sigma_{b,i}$ and $\sigma_{c,i}$ are coefficients describing the distribution of the increase in total stress as a function of depth. For rectangular, trapezoidal and triangular distributions, the values of $\sigma_{a,i}$, $\sigma_{b,i}$ and $\sigma_{c,i}$ can be readily derived from Eq. (8) according to the values of stress increase at $z = 0$ and $z = h$, as presented in Figs. 2(b)-2(d). For a parabolic distribution as shown in Fig. 2(e), $\sigma_{a,i} \neq 0$ and $\sigma_{c,i} = \sigma_i$ at $z = 0$, and $\sigma_{b,i}$ can be specified.

Eqs. (1)-(10) are the mathematical description of two-dimensional free strain consolidation with sand blankets under multi-ramp loading.

3. Analytical solution

3.1 Consolidation of clay layers

The excess pore-water pressure of soil can be expressed by introducing the Fourier sine and cosine series as follows

$$u(x,z,t)=\sum_{m=1}^{\infty}\sum_{n=1}^{\infty}\left[\cos(\mu_{mn}z)+\eta_{mn}\sin(\mu_{mn}z)\right]\cos(\lambda_m x)T_{mn}(t) \tag{11}$$

where

$$\eta_{mn}=\frac{k_{d1}h_1\lambda_m^2}{k_v\mu_{mn}} \tag{12}$$

$$\lambda_m=\frac{(2m-1)\pi}{2l},\ m=1,2,3..... \tag{13}$$

where λ_m, η_{mn} and μ_{mn} are coefficients to be determined. μ_{mn} can be derived by substituting Eqs. (12) and (13) into Eq. (14)

$$\left[k_{d1}h_1\lambda_m^2\cos(\mu_{mn}h)-k_v\mu_{mn}\sin(\mu_{mn}h)\right]+k_{d2}h_2\lambda_m^2\left[\cos(\mu_{mn}h)+\eta_{mn}\sin(\mu_{mn}h)\right]=0 \tag{14}$$

By introducing the Fourier sine and cosine series, Eq. (6) can be expressed as

$$\sigma(x,z,t)=\sum_{m=1}^{\infty}\sum_{n=1}^{\infty}\left\{\sum_{i=1}^{K}\left[F_i(t)\left(\sigma_{mn,i}-\sigma_{mn,i-1}\right)\right]\right\}\cos(\lambda_m x)\left[\cos(\mu_{mn}z)+\eta_{mn}\sin(\mu_{mn}z)\right] \tag{15}$$

where $\sigma_{mn,i}$ is the corresponding Fourier coefficient

$$\sigma_{mn,i}=\frac{\int_0^h\int_0^l\sigma_i(x,z)\cos(\lambda_m x)\left[\cos(\mu_{mn}z)+\eta_{mn}\sin(\mu_{mn}z)\right]\mathrm{d}x\mathrm{d}z}{\int_0^h\int_0^l\left[\cos(\lambda_m x)\right]^2\left[\cos(\mu_{mn}z)+\eta_{mn}\sin(\mu_{mn}z)\right]^2\mathrm{d}x\mathrm{d}z} \tag{16}$$

Substituting Eq. (8) into Eq. (16), the following equations can be derived

$$\sigma_{mn,i}=\frac{2}{l\lambda_m\theta_{mn}}(-1)^{m+1}\cdot\left\{\theta_{1mn,i}+\theta_{2mn,i}+\theta_{3mn,i}+\eta_{mn}\left[\theta_{4mn,i}+\theta_{5mn,i}+\theta_{6mn,i}\right]\right\} \tag{17}$$

$$\theta_{1mn,i}=\frac{\sigma_{a,i}}{\mu_{mn}^3}\left[h^2\mu_{mn}^2\sin\left(\mu_{mn}h\right)+2h\mu_{mn}\cos\left(\mu_{mn}h\right)-2\sin\left(\mu_{mn}h\right)\right] \tag{18}$$

$$\theta_{2mn,i}=\frac{\sigma_{b,i}}{\mu_{mn}^2}\left[h\mu_{mn}\sin\left(\mu_{mn}h\right)+\cos\left(\mu_{mn}h\right)-1\right] \tag{19}$$

$$\theta_{3mn,i}=\frac{\sigma_{c,i}}{\mu_{mn}}\sin\left(\mu_{mn}h\right) \tag{20}$$

$$\theta_{4mn,i}=\frac{\sigma_{a,i}}{\mu_{mn}^3}\left\{2\left[\cos\left(\mu_{mn}h\right)-1\right]+2h\mu_{mn}\sin\left(\mu_{mn}h\right)-h^2\mu_{mn}^2\cos\left(\mu_{mn}h\right)\right\} \tag{21}$$

$$\theta_{5mn,i}=\frac{\sigma_{b,i}}{\mu_{mn}^2}\left[\sin\left(\mu_{mn}h\right)-h\mu_{mn}\cos\left(\mu_{mn}h\right)\right] \tag{22}$$

$$\theta_{6mn,i}=\frac{\sigma_{c,i}}{\mu_{mn}}\left[1-\cos\left(\mu_{mn}h\right)\right] \tag{23}$$

$$\theta_{mn}=\left\{2h\mu_{mn}\left[1+\eta_{mn}^2\right]+\left[1-\eta_{mn}^2\right]\sin\left(2\mu_{mn}h\right)+2\eta_{mn}\left[1-\cos\left(2\mu_{mn}h\right)\right]\right\}\Big/4\mu_{mn} \tag{24}$$

Substituting Eqs. (11) and (15) into Eq. (1), the following equations can be obtained

$$-\left[c_{\mathrm{h}}\lambda_m^2+c_{\mathrm{v}}\mu_{mn}^2\right]T_{mn}\left(t\right)=-\left[\phi_{mn}\left(t\right)-\frac{\partial T_{mn}\left(t\right)}{\partial t}\right] \tag{25}$$

where

$$c_{\mathrm{h}}=\frac{k_{\mathrm{h}}}{m_{\mathrm{v}}\gamma_{\mathrm{w}}} \tag{26}$$

$$c_{\mathrm{v}}=\frac{k_{\mathrm{v}}}{m_{\mathrm{v}}\gamma_{\mathrm{w}}} \tag{27}$$

$$\phi_{mn}\left(t\right)=\sum_{i=1}^{K}\frac{1-H\left\langle t-t_{i,1}\right\rangle}{t_{i,1}-t_{i,0}}H\left\langle t-t_{i,0}\right\rangle\left(\sigma_{mn,i}-\sigma_{mn,i-1}\right) \tag{28}$$

Based on Eq. (25), the following equations can be derived

$$T_{mn}\left(t\right)=a_{mn}\mathrm{e}^{-\rho_{mn}t}+\frac{1}{\rho_{mn}}\phi_{mn}\left(t\right) \tag{29}$$

where

$$\rho_{mn}=\left(c_{\mathrm{h}}\lambda_m^2+c_{\mathrm{v}}\mu_{mn}^2\right) \tag{30}$$

Substituting Eq. (29) into Eq. (11) yields

$$u\left(x,z,t\right)=\sum_{m=1}^{\infty}\sum_{n=1}^{\infty}\cos(\lambda_m x)\left[a_{mn}\mathrm{e}^{-\rho_{mn}t}+\frac{1}{\rho_{mn}}\phi_{mn}\left(t\right)\right]\left[\cos(\mu_{mn}z)+\eta_{mn}\sin(\mu_{mn}z)\right] \tag{31}$$

Substituting Eq. (31) into initial condition Eq. (10) and combining Eq. (28), the following equation can be derived

$$a_{mn}=-\frac{1}{\rho_{mn}}\frac{\sigma_{mn,1}}{t_{1,1}-t_{1,0}},\quad t_{1,0}\le t<t_{1,1} \tag{32}$$

According to the continuity condition of pore water pressure at the inflection points of loading time t ($t_{1,1}$, $t_{2,0}$, $t_{2,1}$…as shown in Fig. 2), the pore pressure is expressed as

$$u\left(x,z,t\right)=\sum_{m=1}^{\infty}\sum_{n=1}^{\infty}\frac{1}{\rho_{mn}}C_{mn}\left(t\right)\cos(\lambda_m x)\left[\cos(\mu_{mn}z)+\eta_{mn}\sin(\mu_{mn}z)\right] \tag{33}$$

where

$$C_{mn}\left(t\right)=\sum_{i=1}^{K}\frac{\sigma_{mn,i}-\sigma_{mn,i-1}}{t_{i,1}-t_{i,0}}\left[\mathrm{e}^{-\rho_{mn}\left(t-t_{i,1}\right)H\left\langle t-t_{i,1}\right\rangle}-\mathrm{e}^{-\rho_{mn}\left(t-t_{i,0}\right)H\left\langle t-t_{i,0}\right\rangle}\right] \tag{34}$$

3.2 Solutions for excess pore-water pressure

ρ_{mn} can be derived by substituting λ_m, μ_{mn} into Eq. (30). Combining Eqs. (12) and (34), then the solution of excess pore water pressure of soil at any point at any time (i.e., Eq. (33)) can be solved.

Based on Eq. (1), the average excess pore water pressure can be obtained:

$$\begin{aligned}\bar{u}&=\frac{1}{lh}\int_0^h\int_0^l u\left(x,z,t\right)\mathrm{d}x\mathrm{d}z\\&=\frac{1}{lh}\sum_{m=1}^{\infty}\sum_{n=1}^{\infty}\frac{\left(-1\right)^{m+1}C_{mn}\left(t\right)}{\lambda_m\mu_{mn}\rho_{mn}}\left\{\sin\left(\mu_{mn}h\right)+\eta_{mn}\left[1-\cos\left(\mu_{mn}h\right)\right]\right\}\end{aligned} \tag{35}$$

3.3 Degree of consolidation

As usual, the overall average degree of consolidation is defined as follows

$$U\left(t\right)=\frac{\frac{1}{lh}\int_0^h\int_0^l m_{\mathrm{v}}\left[\sigma\left(x,z,t\le t_{K+1,0}\right)-u\left(x,z,t\right)\right]\mathrm{d}x\mathrm{d}z}{\frac{1}{lh}\int_0^h\int_0^l m_{\mathrm{v}}\sigma_K\left(x,z,t_{K,1}\right)\mathrm{d}x\mathrm{d}z} \tag{36}$$

Based on Eqs. (6) to (9), the following equations can be obtained

$$\int_0^h\int_0^l\sigma\left(x,z,t\le t_{K+1,0}\right)\mathrm{d}x\mathrm{d}z=\sum_{i=1}^{K}F_i\left(t\right)l\cdot\left[\frac{\sigma_{a,i}-\sigma_{a,i-1}}{3}h^3+\frac{\sigma_{b,i}-\sigma_{b,i-1}}{2}h^2+\left(\sigma_{c,i}-\sigma_{c,i-1}\right)h\right] \tag{37}$$

$$\int_0^h\int_0^l\sigma_K\left(x,z,t_{K,1}\right)\mathrm{d}x\mathrm{d}z=l\left(\frac{\sigma_{a,K}}{3}h^3+\frac{\sigma_{b,K}}{2}h^2+\sigma_{c,K}h\right) \tag{38}$$

Thus, by substituting Eqs. (34), (37) and (38) into Eq.

Table 1 Physical and mechanical indexes and loading mode of soil and sand blanket

Stage	Loading mode	Soil properties	Drain properties
Stage 1 (before 4500 days)	σ_1 = 8.5 kPa; $t_{1,1}$ = 240 d; $t_{2,0}$ = 690 d; σ_2 = 92 kPa; $t_{2,1}$ = 2200 d; $t_{3,0}$ = 3300 d; σ_3 = 116 kPa; $t_{3,1}$ = 3630 d; $t_{4,0}$ = 4500 d	$k_v = k_h = 9.0\times10^{-5}$ m/day; $m_v = 1.7\times10^{-4}$ kPa^{-1}	$k_{d1} = 2.16\times10^{1}$ m/day
Stage 2 (after 4500 days)	σ_4 = 260 kPa; $t_{4,1}$ = 4850 d	$k_v = k_h = 5.0\times10^{-5}$ m/day; $m_v = 5.2\times10^{-4}$ kPa^{-1}	$k_{d1} = 2.16\times10^{1}$ m/day

(36), the overall average degree of consolidation can be obtained.

4. Verification

To verify the accuracy and validity of the proposed analytical solution, the solutions presented in this paper are compared with the measured data of Ma12 layer of Sakishima Reclaimed Island (Mimura and Jang 2005). The specific geometric parameters of Ma12 layer and upper and lower sand blankets are: L = 1000 m, H = 11 m, $2h_1$ = 9 m, $2h_2$ =15m. Physical and mechanical indexes of the clay layer and sand blankets are divided into stage 1 and stage 2 by the time node. Clay has been consolidated in stage 1 before applying the loading of stage 2. All involved parameters are presented in Table 1.

The elasto-viscoplastic finite element analysis was carried out by Mimura and Jang (2005) to assess the long-term settlement for Sakishima Reclaimed Island. One-dimensional analysis was adopted in the finite element analysis considering the extensive reclaimed area and approximately drained condition of sand blankets sandwiched by the clay layer. Thus, the side boundaries of the gravelly sand layers were assumed to be perfectly drained while the side boundary of the clay layer was set to be fully undrained. In this study, however, the two-dimensional consolidation analysis is carried out by considering both the horizontal and vertical seepage of the clay layer. The side boundaries of the clay and sand blankets are set as drained, as described in Eq. (3). Due to the huge length of the clay layer, the vertical seepage predominates the whole consolidation process while the horizontal seepage may be negligible. As a result, there will be no significant difference between the one-dimensional analysis and two-dimensional analysis.

Fig. 3 shows the ground settlement development with time, along with the in-situ measured data and finite element results of Mimura and Jang (2005). It suggests that the trend of settlement change in this study is highly consistent with the measured data and finite element results, and the final settlement is the same. Compared with measure data and finite element results, the settlement in this study increases rapidly in Stage 2. It may be attributed to the use of constant hydraulic conductivity in this study. In fact, the actual hydraulic conductivity of clay decreases gradually with time during soil consolidation process. In the finite element analysis, the hydraulic conductivity was assumed to change with the void ratio. As contrast, for analysis purposes, the average hydraulic conductivity is adopted in the proposed analytical solution, which is larger

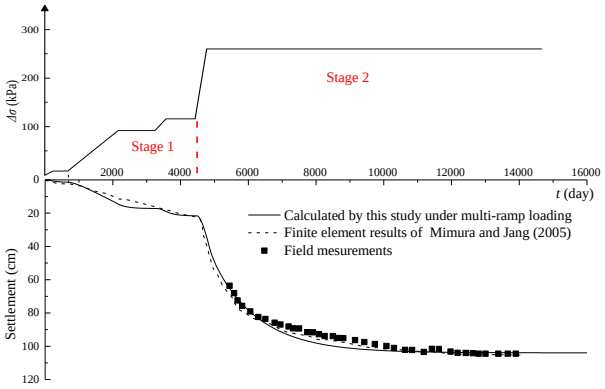

Fig. 3 Comparison of the calculated settlement with finite element results and measured data

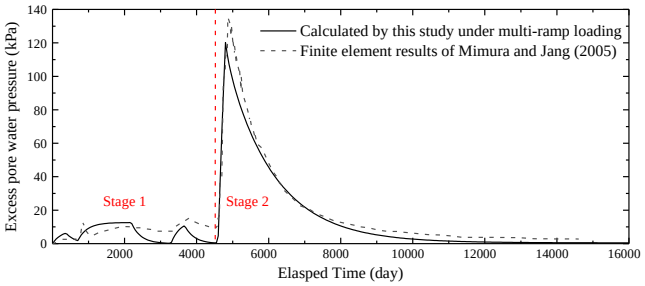

Fig. 4 Comparison of the calculated settlement with finite element results and measured data

than the actual value in Stage 2. As a result, the settlement develops rapidly during the initial period of Stage 2 compared to the results of field measurement and finite element analysis. However, it does not influence the accuracy of the calculated final settlement.

In addition, the generation-dissipation process of excess pore water pressure is also calculated and compared with the finite element results of Mimura and Jang (2005), as shown in Fig. 4. A good agreement can be obtained between the two results. In conclusion, through the comparison of the settlement and pore water pressure, the proposed solution in this study proves to be efficient and accurate to solve the two-dimensional consolidation problem with sand blankets under multi-ramp loading.

5. Results and discussion

For analysis purposes, in section, physical and mechanical parameters and geo-metric dimensions of soils in Ma12 layer of Sakishima Reclaimed Island in Table 1 and Fig. 1 are adopted for the subsequent analysis and discussion unless otherwise stated, such as L = 1000 m, h =

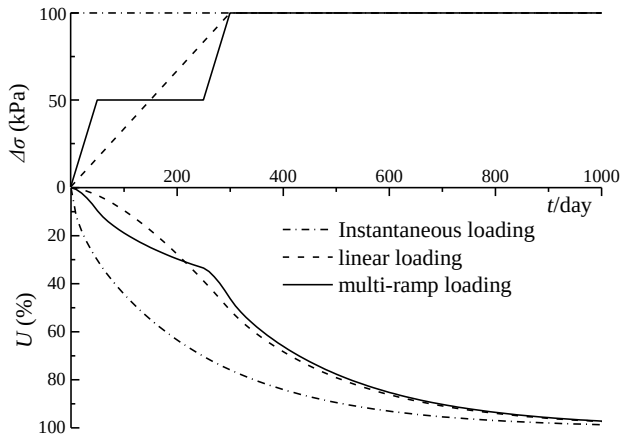

Fig. 5 Effect of loading mode on the degree of consolidation

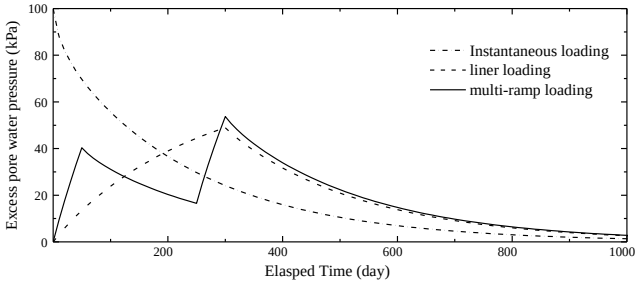

Fig. 6 Effect of loading mode on the generation-dissipation process of excess pore water pressure

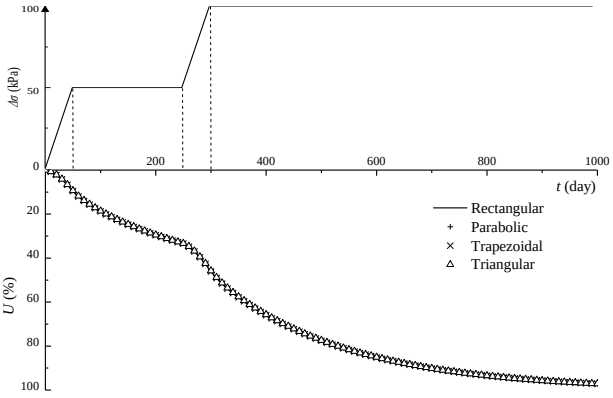

Fig. 7 Effect of stress distribution on the degree of consolidation

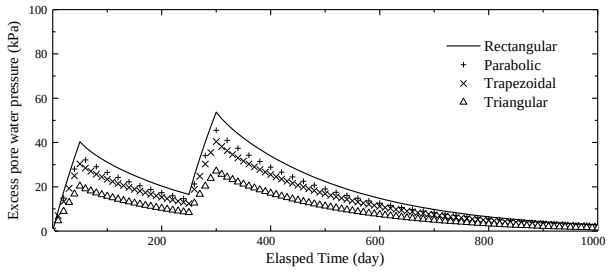

Fig. 8 Effect of stress distribution on the generation-dissipation process of excess pore water pressure

11 m, $2h_1$ = 9 m, $2h_2$ =15m; $m_v = 1.7\times10^{-4}$ kPa^{-1}, $k_v = k_h = 9.53\times10^{-5}$ m/day, $k_{d1} = k_{d2} = 2.16\times10^{1}$ m/day (Mimura and Jang 2005).

5.1 Effect of loading mode on soil consolidation

To analyze the influence of the loading mode on soil consolidation, three different loading modes are considered: instantaneous loading ($t_{1,1}$ = 0, σ_1 = 100 kPa), linear loading (σ_1 = 100 kPa, $t_{1,1}$ = 300 d) and multistage loading (taking two-stage loading as an example σ_1 = 50 kPa, $t_{1,1}$ = 50 d, $t_{2,0}$ = 250 d, $t_{2,1}$ = 300 d and σ_2 = 100 kPa). The consolidation and pore pressure dissipation processes under the three different loading modes are presented in Figs. 5 and 6, respectively. As expected, the consolidation rate and pore pressure dissipation rate of instantaneous loading are significantly faster than those of linear loading and multi-ramp loading. During the loading period, the consolidation rate of linear loading is faster than that of multi-ramp loading. In contrast, after loading, there is little difference in the degree of consolidation and dissipation rate of pore pressure between them. Evidently, the faster the loading rate, the faster the pore pressure dissipation and consolidation rate.

5.2 Effect of stress distribution on soil consolidation

To investigate the influence of the stress distribution mode on consolidation, four stress distribution modes (i.e., rectangular, triangular, trapezoidal and parabolic distributions as shown in Fig. 2) as a function of depth are considered. Multi-ramp loading as same as that of the previous subsection (i.e., σ_1 = 50 kPa, $t_{1,1}$ = 50 d; $t_{2,0}$ = 250 d; σ_2 = 100 kPa, $t_{2,1}$ = 300 d) is adopted here, as shown in Fig. 7. In the following subsections, the same loading mode are considered when investigating the effect of hydraulic conductivity and thickness of sand blanket on soil consolidation. Fig. 7 shows that there is almost no difference among calculated degrees of consolidation for the four stress distribution modes. As can be seen from Fig. 8, however, the generation-dissipation processes of excess pore water pressure for the four stress distribution modes are significantly different. For the rectangular stress distribution, the excess pore water pressure generated is largest, and it needs more to dissipate completely. In contrast, the excess pore water pressure for the triangular distribution is smallest and dissipates promptly. In conclusion, the effect of the stress distribution mode on the consolidation rate is insignificant and may be neglected. However, special attention should be paid to its effect on the generation and dissipation process of excess pore water pressure.

5.3 Effect of hydraulic conductivity of sand blanket on soil consolidation

Hydraulic conductivity of the sand blanket is an important parameter, which significantly affects the soil consolidation process. To analyze the effect of hydraulic conductivity of the sand blanket, the hydraulic conductivity of the top and bottom sand blankets are set as the same value, that is $k_{d1} = k_{d2} = k_d$. Five types of ratios of hydraulic

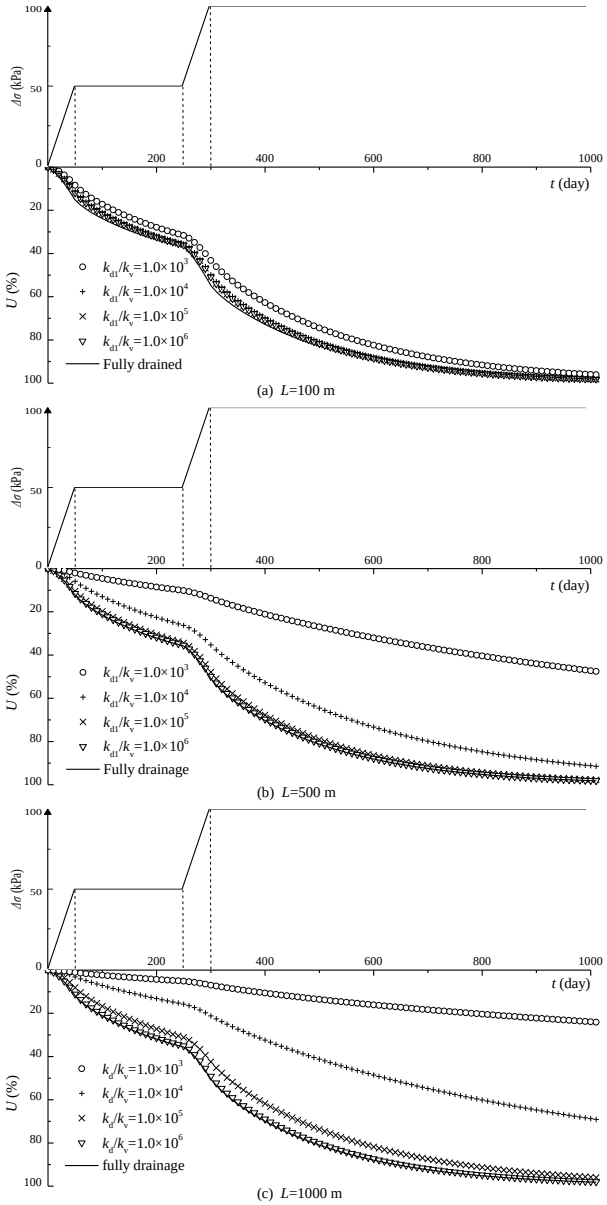

Fig. 9 Effect of hydraulic conductivity of sand blanket on consolidation of soil with various soil widths L

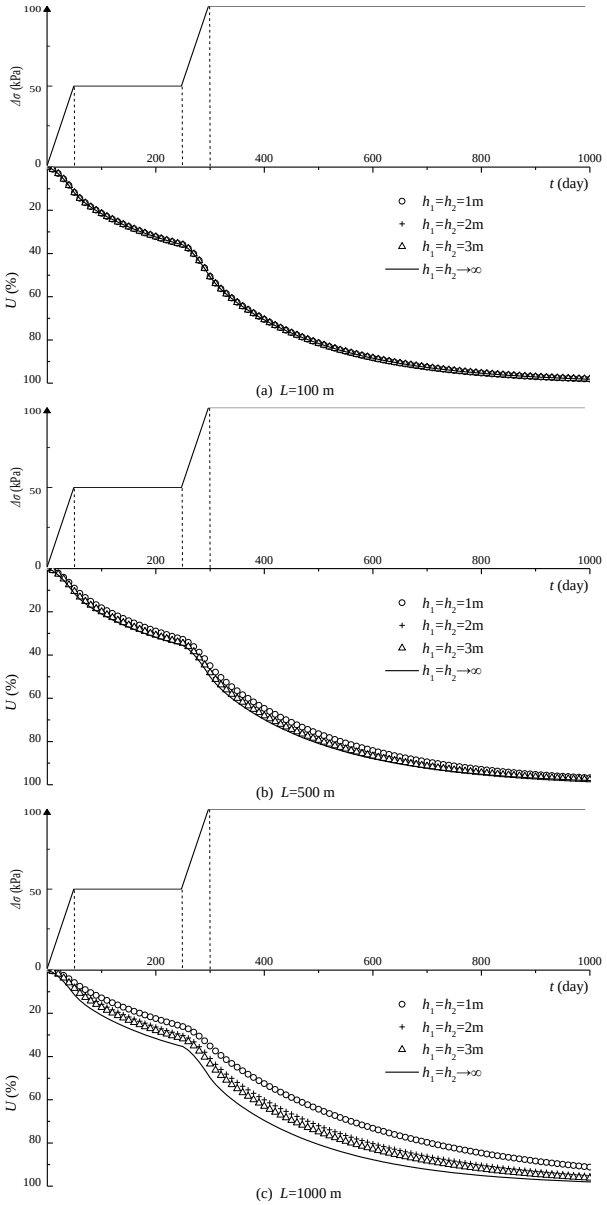

Fig. 10 Effect of thickness of sand blanket on soil consolidation with various soil widths L

conductivity of the sand blanket and clay (i.e., k_d/k_v = 1.0×10^3, 1.0×10^4, 1.0×10^5, 1.0×10^6, 1) are taken into account in this study. Note that when k_d/k_v = 1, the drainage capacity of the sand blanket is enough to discharge the water expelled from clay. Therefore, in this case, the boundary of the sand blanket is considered as the fully drained boundary. In addition, three types of soil widths L (i.e., horizontal seepage path L = 100 m, 500 m and 1000 m) are considered here, as shown in Fig. 9.

It can be seen that when L = 100 m, the results of k_d/k_v = 1.0×10^4 and fully drained condition are very close. It suggests that when k_d/k_v = 1.0×10^4, the sand blanket has reached the requirement of fully drained condition. In contrast, when L increases to 500 m and 1000 m, the value of k_d/k_v should be greater than 1.0×10^5 and 1.0×10^6, respectively, to meet the requirement of fully drained conditions. It indicates that different soil widths lead to different values of hydraulic conductivity of sand blankets to reach fully drained conditions. The larger soil width means that pore water needs to travel a longer distance to be discharged from the soil. As a result, a larger hydraulic conductivity of the sand blanket is needed to guarantee the smooth flow of the expelled water with little resistance in the sand blanket.

5.4 Effect of hydraulic conductivity of sand blanket on soil consolidation

Fig. 10 shows the effect of thickness of sand blanket with various lengths L on soil consolidation. Four different thicknesses (i.e., h_1 = h_2 = 1 m, 2 m, 3 m and ∞) are considered. When the length of sand blanket is relatively small, such as L = 100 m, there is almost no visible difference among the four thicknesses, as shown in Fig.

10(a). However, as L increases, the influence of thickness of sand blanket on consolidation becomes evident gradually. Especially, when L = 1000 m, as can be seen from Fig. 10(c), the consolidation rate for $h_1 = h_2 = \infty$ is much faster than that for $h_1 = h_2 = 1$ m.

This phenomenon can be explained from the relationship between the drainage efficiency and size of sand blanket. The larger the thickness of sand blanket, the faster the water can be discharged from the soil to be consolidated through the sand blanket. When L is small, the horizontal seepage path during consolidation is short. In this case, the water can be drained smoothly through the sand blanket, even when the sand blanket is very thin, e.g., $h_1 = h_2 = 1$ m. In such case, the boundary can be regarded as the fully drain boundary. As L increases, the water discharged from the soil needs to travel a longer distance to reach the free drained boundary. Therefore, the sand blanket with a thin thickness will limit the drainage of water. As a result, the larger the thickness of sand blanket, the faster the consolidation rate, as shown in Fig. 10(c).

6. Conclusions

In this paper, an analytical solution is proposed for the two-dimensional consolidation problem with horizontal sand blankets under multi-ramp loading. After validation of the solution, the influence of the loading mode, stress distribution mode, hydraulic conductivity and thickness of the sand blanket on consolidation are analyzed. The concluding remarks can be drawn as follows:

• Different loading modes have a significant influence on soil consolidation. The faster the loading rate, the faster the consolidation rate and pore pressure dissipation rate of instantaneous loading. Compared with instantaneous and linear loading, multi-ramp loading may considerably prolong the whole soil consolidation process.

• The stress distribution significantly affects the generation-dissipation process of pore water pressure, while its inflence on soil consolidatoin rate is negligible. This is because that the stress distribution directly affects the distribution of pore pressure with little contribution to the average degree of consolidation of the whole soil.

• To make sure that the sand blanket can be regarded as the fully drained condition, the ratio of hydraulic conductivity of the sand blanket to that of clay layer k_d/k_v should be greater than 1.0×10^4, 1.0×10^5 and 1.0×10^6 with soil width L being 100 m, 500 m and 1000 m, respectively. A larger soil width needs a larger hydraulic conductivity of the sand blanket to guarantee the smooth flow of the expelled water with little resistance in the sand blanket.

• When the length of the sand blanket is relatively small (e.g., L = 100 m), there is almost no visible difference among the consolidation rate under different thicknesses of the sand blanket. However, as L increases, the influence of thickness of sand blanket on consolidation becomes evident gradually.

Acknowledgments

The research was financially supported by the National Natural Science Foundation of China (Grant No. 41972269), and the Jiangsu Provincial Transportation Engineering Construction Bureau (CX-2019GC02).

References

Barron, R.A. (1948), "Consolidation of fine-grained soils by drain wells", *Transactions of the American Society of Civil Engineers*, **113**(1), 718-754. https://doi.org/10.1061/TACEAT.0006098.

Chai, J.C. and Miura, N. (1999), "Investigation of factors affecting vertical drain behavior", *J. Geotech. Geoenviron. Eng.*, **125**(3), 216-226. https://doi.org/10.1061/(ASCE)1090-0241(1999)125:3(216).

Chai, J.C., Horpibulsuk, S., Shen, S. and Carter, J.P. (2014), "Consolidation analysis of clayey deposits under vacuum pressure with horizontal drains", *Geotext. Geomembranes*, **42**(1), 437-444. https://doi.org/10.1016/j.geotexmem.2014.07.001.

Conte, E. and Troncone, A. (2006), "One-dimensional consolidation under general time-dependent loading", *Can. Geotech. J.*, **43**(11), 1107-1116. https://doi.org/10.1139/t06-064.

Feng, J., Ni, P. and Mei, G. (2019), "One-dimensional self-weight consolidation with continuous drainage boundary conditions: Solution and application to clay-drain reclamation", *Int. J. Numer. Anal. Method. Geomech.*, **43**(8), 1634-1652. https://doi.org/10.1002/nag.2928.

Feng, J., Ni, P., Chen, Z., Mei, G. and Xu, M. (2020), "Positioning design of horizontal drain in sandwiched clay-drain systems for land reclamation", *Comput. Geotech.*, **127**, 103777. https://doi.org/10.1016/j.compgeo.2020.103777.

Feng, S., Wang, W., Chen, Z. and Chen, H. (2021), "Analytical solution to consolidation of accreting soil considering step load and horizontal drainage layers", *Mar. Georesour. Geotech.*, **39**(8), 889-905. https://doi.org/10.1080/1064119X.2020.1776802.

Gibson, R.E. and Shefford, G.C. (1968), "The efficiency of horizontal drainage layers for accelerating consolidation of clay embankments", *Géotechnique*, **18**(3), 327-335. https://doi.org/10.1680/geot.1968.18.3.327.

Gray, H. (1945), "Simultaneous consolidation of contiguous layers of unlike compressible soils", *Transactions of the American Society of Civil Engineers*, **110**, 1327-1356.

Indraratna, B., Rujikiatkamjorn, C., Balasubramaniam, A.S. and McIntosh, G. (2012), "Soft ground improvement via vertical drains and vacuum assisted preloading", *Geotext. Geomembranes*, **30**: 16-23. https://doi.org/10.1016/j.geotexmem.2011.01.004.

Jang, W.Y. and Mimura, M. (2005), "Effect of permeability and compressibility of sandwiched gravelly sand layers on subsequent settlement of Pleistocene deposits", *Soils Found.*, **45**(6), 111-119. https://doi.org/10.3208/sandf.45.111.

Lee, M.S. and Oda, K. (2015), "Evaluation of excess pore water pressure characteristics in sand mat used for recycling dredged soil", *Mar. Georesour. Geotech.*, **33**(5), 367-375. https://doi.org/10.1080/1064119X.2014.890985.

Lee, S.L., Karunaratne, G.P., Yong, K.Y. and Ganeshan, V. (1987), "Layered Clay-Sand Scheme of Land Reclamation", *J. Geotech. Eng.*, **113**(9), 984-995. https://doi.org/10.1061/(ASCE)0733-9410(1987)113:9(984).

Lei G., Li, Z. and Xu, L. (2016), "Free-strain solutions for two-dimensional consolidation with sand blankets", *Chinese J. Geotech. Eng.*, **38**(2), 193-201. (in Chinese).

Lei, G., Fu, C. and Ng, C.W.W. (2016), "Vertical-drain consolidation using stone columns: An analytical solution with an impeded drainage boundary under multi-ramp loading", *Geotext. Geomembranes*, **44**(1), 122-131. https://doi.org/10.1016/j.geotexmem.2015.07.003.

Lei, G., Zheng, Q., Ng, C.W.W., Chiu, A.C.F. and Xu, B. (2015), "An analytical solution for consolidation with vertical drains under multi-ramp loading", *Géotechnique*, **65**(7), 531-547. https://doi.org/10.1680/geot.13.P.196.

Li, Z., Lei, G. and Fu, C. (2016), "Free-strain solutions for two-dimensional consolidation with a sand-wall drain", *Rock Soil Mech.*, **37**(6), 1613-1622. (in Chinese).

Liu, J., Lei, G. and Zheng, M. (2014), "General solutions for consolidation of multilayered soil with a vertical drain system", *Geotext. Geomembranes*, **42**(3), 267-276. https://doi.org/10.1016/j.geotexmem.2014.04.001.

Lu, M., Xie, K. and Wang, S. (2011), "Consolidation of vertical drain with depth-varying stress induced by multi-stage loading", *Comput. Geotech.*, **38**(8), 1096-1101. https://doi.org/10.1016/j.compgeo.2011.06.007.

Mesri, G. (1973), "One-dimensional consolidation of a clay layer with impeded drainage boundaries", *Water Resour. Res.*, **9**(4): 1090-1093. https://doi.org/10.1029/WR009i004p01090.

Mesri, G. and Funk, J.R. (2015), "Settlement of the Kansai International Airport Islands", *J. Geotech. Geoenviron. Eng.*, **141**(2), 04014102. https://doi.org/10.1061/(ASCE)GT.1943-5606.0001224.

Mimura, M. and Jang, W.Y. (2004), "Description of time-dependent behavior of quasi-overconsolidated Osaka Pleistocene clays using elasto-viscoplastic finite element analyses", *Soils Found.*, **44**, 41-52. https://doi.org/10.3208/sandf.44.4_41.

Mimura, M. and Jang, W.Y. (2005), "Verification of the elasto-viscoplastic approach assessing the long-term deformation of the quasi-overconsolidated pleistocene clay deposits", *Soils Found.*, **45**(1), 37-49. https://doi.org/10.3208/sandf.45.1_37.

Mimura, M., Takeda, K., Yamamoto, K., Fujiwara, T. and Jang, W.Y. (2003), "Long-term settlement of the reclaimed quasi-over-consolidated Pleistocene clay deposits in Osaka Bay", *Soils Found.*, **43**(6), 141-153. https://doi.org/10.3208/sandf.43.6_141.

Ni, P., Mei, G. and Zhao, Y. (2019), "Surcharge preloading consolidation of reclaimed land with distributed sand caps", *Mar. Georesour. Geotec.*, **37**(6), 671-682. https://doi.org/10.1080/1064119X.2018.1482389.

Nogami, T. and Li, M. (2002), "Consolidation of system of clay and thin sand layers", *Soils Found.*, **42**(4), 1-11. https://doi.org/10.3208/sandf.42.4_1.

Nogami, T. and Li, M. (2003), "Consolidation of clay with a system of vertical and horizontal drains", *J. Geotech. Geoenviron. Eng.*, **129**(9), 838-848. https://doi.org/10.1061/(ASCE)1090-0241(2003)129:9(838).

Tan, S.A., Liang, K.M., Yong, K.Y. and Lee, S.L. (1992), "Drainage efficiency of sand layer in layered clay-sand reclamation", *J. Geotech. Eng.*, **118**(2), 209-228. https://doi.org/10.1061/(ASCE)0733-9410(1992)118:2(209).

Tian, Y., Wu, W., Jiang, G., El Naggar, M.H., Mei, G., Xu, M. and Liang, R. (2020), "One-dimensional consolidation of soil under multistage load based on continuous drainage boundary", *Int. J. Numer. Anal. Method. Geomech.*, **44**(8), 1170-1183. https://doi.org/10.1002/nag.3055.

Yao, R., Ni, P., Mei, G. and Zhao, Y. (2019), "Numerical analysis of surcharge preloading consolidation of layered soils via distributed sand blankets", *Mar. Georesour. Geotec.*, **37**(8), 902-914. https://doi.org/10.1080/1064119X.2018.1506529.

Zhu, G. and Yin, J.H. (2004), "Consolidation analysis of soil with vertical and horizontal drainage under ramp loading considering smear effects", *Geotext. Geomembranes*, **22**(1-2), 63-74. https://doi.org/10.1016/S0266-1144(03)00052-9.

GC